CHARACTERIZATION OF THE ELECTRON ENERGY RELAXATION PROCESS IN NbN HOT-ELECTRON DEVICES

K. S. Il'in, G. N. Gol'tsman,* and B. M. Voronov
Physics Department, Moscow State Pedagogical University, Moscow 119435, Russia
*email: goltsman@rpl.mpgu.msk.su

Roman Sobolewski
Laboratory for Laser Energetics and Department of Electrical and Computer Engineering
University of Rochester, 250 East River Road, Rochester, NY 14623-1299

Abstract

We report on transient measurements of electron energy relaxation in NbN films with 300-fs time resolution. Using an electro-optic sampling technique, we have studied the photoresponse of 3.5-nm-thick NbN films deposited on sapphire substrates and exposed to 100-fs-wide optical pulses. Our experimental data analysis was based on the two-temperature model and has shown that in our films at the superconducting transition 10.5 K the inelastic electron-phonon scattering time was about (10±2) ps. This response time indicated that the maximum intermediate-frequency band of a NbN hot-electron phonon-cooled mixer should reach (16+4/−3) GHz if one eliminates the bolometric phonon-heating effect. We have suggested several ways to increase the effectiveness of phonon cooling to achieve the above intrinsic value of the NbN mixer bandwidth.

Introduction

In the terahertz frequency range, hot-electron mixers (HEM) have reached noise temperatures lower than the other mixer types, such as superconductor–insulator–superconductor tunnel junctions or Schottky diodes. Both Nb diffusion-cooled and NbN phonon-cooled devices demonstrate roughly the same noise temperatures. For a phonon-cooled, 3.5-nm-thick NbN mixer, the 4-GHz gain bandwidth has been demonstrated[1] at 140-GHz and 660-GHz frequencies, and the noise bandwidth at 620 GHz has been found to breach twice the gain bandwidth.[2] For a diffusion-cooled Nb HEM, the 9-GHz gain bandwidth has been measured at 600 GHz.[3]

In the HEM device, the rate of electron cooling controls the bandwidth of the intermediate frequency output; thus, the intrinsic bandwidth of an ideal phonon-cooled HEM corresponds to the inverse of the inelastic electron-phonon scattering time. In real

HEM's, unfortunately, nonequilibrium phonons hamper the device performance. Reabsorption of excited phonons by electrons slows the electron cooling, leading to the increased response time and the decrease of the HEM bandwidth. This explains why numerous experimental studies of NbN ultrathin HEM's resulted in a measured bandwidth smaller than one would expect from the value of the electron-phonon scattering time determined in independent experiments. Thus, secondary processes, such as phonon reabsorption and phonon escape from the film to the substrate, directly affect the results of frequency-domain HEM measurements.

In this work, we report our direct measurements of the electron energy relaxation time in a 3.5-nm-thick NbN HEM using a time-domain electro-optic (EO) sampling technique with 300-fs resolution.[4] EO sampling does not require the response signal to be transmitted out of the cryostat; instead, the signal is measured *in situ*, in the close vicinity (less than 100 μm) to HEM integrated into a coplanar waveguide. As compared to frequency-domain methods, EO sampling provides much more accurate data on the intrinsic picosecond response of the device. Our studies show that the intrinsic gain bandwidth of the NbN HEM is up to 16 GHz, which is sufficient for most coherent terahertz detection applications.

Experimental

Films with a 3.5-nm thickness were deposited on sapphire substrates by reactive dc magnetron sputtering in the Ar+N_2 gas mixture.[5] The largest values of both the critical current density J_c and the transition temperature T_c were achieved at the discharge current of 300 mA, the partial N_2 pressure of 1.1×10^{-4} mbar, and the substrate temperature 850°C. The Ar pressure proved to have no substantial impact on the film deposition rate or film composition, and for this reason, the 4.8×10^{-3}-mbar pressure was selected to maintain a stable discharge. The deposition rate was 0.5 nm/s, defined as the ratio between the film thickness (measured with a mechanical profilometer) and the deposition time.

A typical experimental configuration, used for the EO sampling measurements, is shown in Fig. 1. The test structure was patterned into a 4-mm-long coplanar waveguide (CPW) with a 30-μm-wide central line, separated by 5-μm-wide gaps from the ground planes. The tested HEM consisted of 25 parallel, 2-μm-wide strips, located in the middle of the CPW, between the central line and grounds. Vanadium strips terminated both ends of the CPW to assure 50-Ω output impedance of our device. Typically, after processing, the device exhibited the midpoint of the superconducting transition (definition of T_c) at 10.3 K, with ~1.0-K transition width, and a critical current density J_c at 4.2 K of 10^6 A/cm^2.

The sample was mounted on a copper cold finger inside an exchange-gas, liquid-helium dewar, with optical access through a pair of fused-silica windows. During our measurements, the sample was in the He exchange gas with the temperature regulated in the range from 4.2 K to 12 K and stabilized to 0.2 K. One end of the CPW was grounded, while the other was wire-bounded directly to a 50-Ω coaxial cable connected through a bias-tee to the 14-GHz sampling oscilloscope. To facilitate EO measurements the entire waveguide structure was overlaid with an electro-optical $LiTaO_3$ crystal.

A block diagram of our experimental setup is shown in Fig. 2 and described in detail in Ref. 4. A commercial self-mode-locked $Ti:Al_2O_3$ laser, pumped by an Ar-ion laser, was used to excite picosecond pulses in the HEM and, simultaneously, to electro-optically measure the resulting electrical transient propagating in the CPW line. The laser provided a train of ~100-fs-wide optical pulses with 800-nm wavelength and 76-MHz repetition rate at an average power of >1 W. The train was split into two beams by a 70/30 beamsplitter. The first (excitation) beam was frequency doubled in a nonlinear crystal, intensity modulated, and focused by a microscope objective to an ~100-μm-diam spot to excite the HEM structure. The microscope objective was also a part of the viewing arrangement that allowed us to observe the sample during beam positioning. The average power of the 400-nm excitation beam measured outside the dewar was ~0.75 mW. By calculating the amount of light absorbed and reflected by two dewar windows and the $LiTaO_3$ crystal, as well as taking into account reflectivity and transmissivity of the NbN film, we estimate that the power actually absorbed by the HEM was only 4.5 μW, which is equivalent to approximately 1.5×10^{16} 3-eV photons per cm^3, and induced below 0.1 K permanent heating of the device area. The second (sampling) beam traveled through a computer-controlled delay line and was focused to a < 10-μm-diam spot inside the $LiTaO_3$ at the gap between the center and ground CPW lines, less than 100 μm from the HEM (see Fig. 1). The transient birefringence introduced in the $LiTaO_3$ crystal by the electric field associated with the HEM photoresponse was detected by the sampling beam, which allowed us to measure the time evolution of the photoresponse voltage signal.[4] From the operational point of view our EO system can be regarded as a sampling oscilloscope featuring <200-fs time resolution and <150-μV voltage sensitivity, which are well below the characteristics of the transients reported here.

Results and Discussion

A typical response of our device measured with our EO-sampling technique is presented in Fig. 3. We note that the signal (solid line) contained a large amount of noise, but it was acquired at low bias current, 175 μA, and at temperature 10.5 K, right at the superconducting-resistive transition. The dashed-dotted line represents the response of the sample calculated for the single-pulse input on the basis of the two-temperature (2T) model.[6] Since the reflection-free time window for our experiments, due to limited length of the CPW and large signal propagation velocity on sapphire, was only about 40 ps, the reflections from the CPW ends contributed to the measured EO sample response and had to be included in simulations. The dashed line in Fig. 3 shows the result of our 2T model calculations that took those reflections into account.

The 2T model assumes a very short thermalization time of quasiparticles. Fast thermalization occurs at high energies via both electron-electron interactions and electron-optical-phonon scattering, while at low energies it is mainly due to electron-electron scattering. For phonons the single-temperature approximation remains reasonable for a relatively weak coupling between phonons and the substrate. For low-temperature superconductors, it is well known that establishment of the phonon nonequilibrium temperature occurs via electron-phonon interactions.

In our simulations, we considered a superconducting film carrying a constant current that drives the sample into the resistive state at the temperature T_b very close to T_c. Under this condition the energy gap is very small as compared to $k_B T_b$, and the quasiparticle energy spectrum is close to that of electrons in a normal metal. Consequently, the inelastic scattering of quasiparticles, as well as their recombination into Cooper pairs, can be described by the electron-phonon interaction time. We assume that the film is uniformly illuminated by radiation and that the bias current is uniformly distributed over the bridge's cross-section area. We also neglect joule heating by the biasing current and consider only small deviations from equilibrium.

The time-dependent effective temperatures T_e and T_{ph} are obtained as a solution of the 2T coupled linear heat-balance equations:

$$C_e \frac{dT_e}{dt} = \frac{\alpha P_{in}(t)}{V} - \frac{C_e}{\tau_{e-ph}} \left(T_e - T_{ph}\right),$$

$$C_{ph} \frac{dT_{ph}}{dt} = \frac{C_{ph}}{\tau_{ph\text{-}e}} \left(T_e - T_{ph}\right) - \frac{C_{ph}}{\tau_{es}} \left(T_{ph} - T_b\right), \qquad (1)$$

where C_e and C_{ph} are the electron and phonon specific heats, α is the radiation absorption coefficient, V is the volume of the bridge, and T_b is the sample temperature. $P_{in}(t)$ is the incident optical power, in our case modeled as a Gaussian-shaped pulse. The equations also contain the characteristic times $\tau_{e\text{-ph}}$ for electron-phonon scattering, and τ_{es} for phonon escape to the substrate. The energy balance equation is $\tau_{e-\text{ph}} = \tau_{\text{ph}-e}\left(C_e/C_{\text{ph}}\right)$, where $\tau_{\text{ph-}e}$ is phonon-electron scattering time. To obtain the corresponding time evolution of the device voltage response, we invoked the methods described in detail in Ref. 6.

A diagram of energy relaxation processes taking place in a metal film under the influence of the electromagnetic radiation is presented in Fig. 4. For the ideal $\tau_{e\text{-ph}} << \tau_{\text{ph-}e}$ and $\tau_{es} << \tau_{\text{ph-}e}$ case, the electron energy relaxation back to equilibrium is essentially due to the inelastic electron scattering with phonons. Thus, the voltage signal decay should occur according to the exponential law with a single characteristic time constant $\tau_{e\text{-ph}}$. For real NbN films at $T \approx 10$ K, $C_e = 1.7 \times 10^{-3}$ J cm^{-3} K^{-1}, and $C_{ph} = 1.1 \times 10^{-2}$ J cm^{-3} K^{-1}, which leads to $\tau_{\text{ph-}e} = 6.5\ \tau_{e\text{-ph}}$. In addition, $\tau_{es} = 13 \times d$(nm) ps, which for our 3.5-nm-thick films results in $\tau_{\text{ph-}e} = 1.7\ \tau_{es}$. Consequently, in our case, the energy flow from electrons to phonons dominates over the re-absorption of nonequilibrium phonons by electrons; however, the energy backflow cannot be neglected. Compared to the ideal device, the shape of the response for a real HEM has a more complicated waveform that cannot be described by the single-time-constant exponential law. In this case, it is only possible to determine the "average" decay time (see Fig. 3), which is given by the time that elapses from the pulse arrival until the magnitude of the response decreases down to $1/e$ from its maximum value. Using this criterion, we obtained for our device the 30-ps relaxation time which corresponds to the HEM gain bandwidth of 5.3 GHz.

The $\tau_{e\text{-ph}}$ value was obtained as the fitting parameter in the 2T equations, which provided the best agreement (dotted and dashed lines in Fig. 4) with the experimental transient and was determined to be (10±2) ps. This value can be regarded as the intrinsic electron-phonon scattering time and limits the maximum gain bandwidth of the 3.5-nm-thick phonon-cooled NbN HEM's to (16+4/–3) GHz.

There are several possible ways to increase the current experimental 5.3-GHz bandwidth limit to the intrinsic 16-GHz value. Further technological development of NbN film deposition (e.g., epitaxial growth) should result in decreased film thickness without degrading its operational parameters, such as T_c and J_c. This should increase the escape rate of nonequilibrium phonons from the film. Phonon escape τ_{es} also depends on the transparency of the film–substrate interface; using substrate materials that provide better acoustic matching with NbN films (e.g., MgO) one would additionally lower τ_{es}. Out-diffusion of hot electrons into the metal contact pads bounded to the superconducting

bridge is commonly used in Nb devices (so-called diffusion-cooled HEM's) to increase their gain bandwidth.[7] The same approach could be implemented for NbN structures, despite NbN's very small electron diffusivity. Finally, it might be beneficial to deposit an acoustically matched, low-loss dielectric layer on top of the device to act as an additional channel for the phonon escape.

Conclusions

We have measured the 30-ps photoresponse of NbN ultrathin films at 10 K and calculated the corresponding (10±2)-ps inelastic electron-phonon scattering time. This latter value imposes the fundamental limit of (16±4/−3) GHz to the intermediate frequency bandwidth of phonon-cooled NbN HEM's. We have also indicated the possible ways to approach this maximal bandwidth in real devices.

Acknowledgment

This work has been supported by Russian Program on Condensed Matter (Superconductivity Division) under Grant N 98062, the U.S. Office of Naval Research Grant N00014-97-1-0696, and the NATO Linkage Grant CRG.LG974662.

References

1. S. Cherednichenko, P. Yagoubov, K. Il'in, G. Gol'tsman, and E. Gershenzon, in *The Proceedings of the 8th International Symposium on Space Terahertz Technology* (Cambridge, MA, 1997), p. 245.
2. H. Ekström, E. Kollberg, P. Yagoubov, G. Gol'tsman, E. Gershenzon, S. Yngvesson, Appl. Phys. Lett. **70** (24), 3296–3298 (1997).
3. B. S. Karasik, A. Scalare, R. A. Wyss, W. R. McGrath, B. Bumble, H. G. LeDuc, J. B. Barner, and A. W. Kleinsasser, Proceedings of the 6th International Conference on Terahertz Electronics, Leeds, UK, September 1998, in press.
4. M. Lindgren, M. Currie, C. A. Williams, T. Y. Hsiang, P. M. Fauchet, R. Sobolewski, S. H. Moffat, R. A. Hughes, J. S. Preston, F. A. Hegmann, IEEE J. Sel. Top. Quantum Electron. **2** (3), 668–678 (1996).
5. P. Yagoubov, G. Gol'tsman, B. Voronov, L. Seidman, V. Siomash, S. Cherednichenko, and E. Gershenzon, "The Bandwidth of HEB Mixers Employing Ultrathin NbN Films on Sapphire Substrate," in *The Proceedings of the 7th International Symposium on Space Terahertz Technology*, (Charlottesville, VA, 1996), p. 290.
6. A. D. Semenov, R. S. Nebosis, Yu. P. Gousev, M. A. Heusinger, K. F. Renk, Phys. Rev. B **52** (1), 581–590 (1995).
7. D. E. Prober, Appl. Phys. Lett. **62** (17), 2119–2121 (1993).

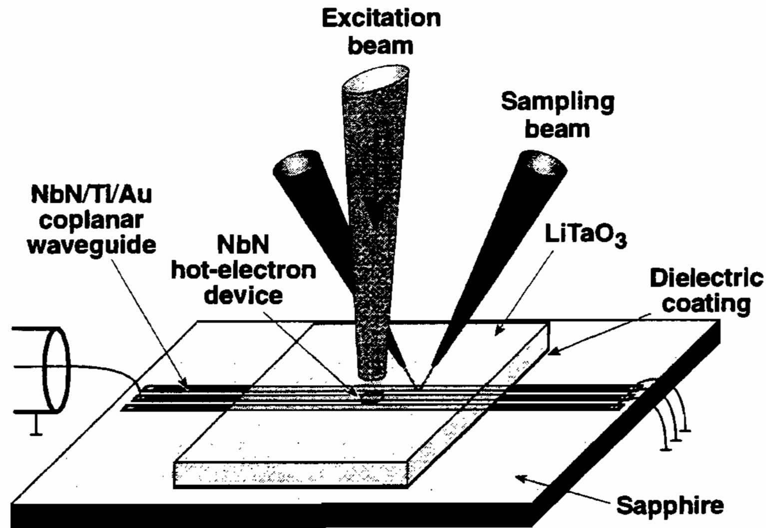

Fig. 1. Experimental configuration for EO sampling testing of a NbN HEM.

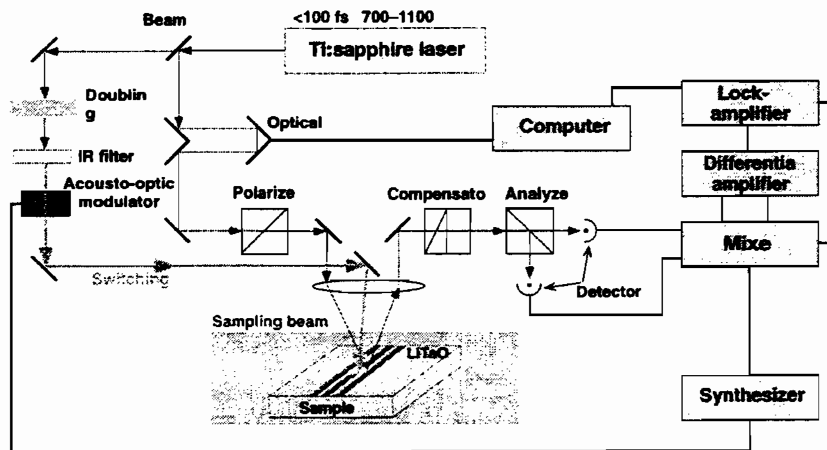

Fig. 2. Block diagram of the EO sampling system.

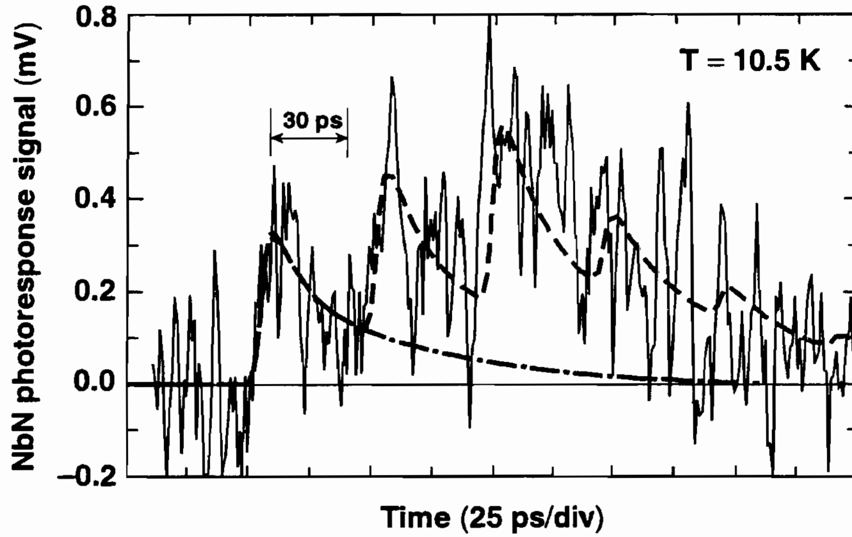

Fig. 3. Time-resolved response of a NbN HEM to a 100-fs optical excitation pulse. Temperature was 10.5 K.

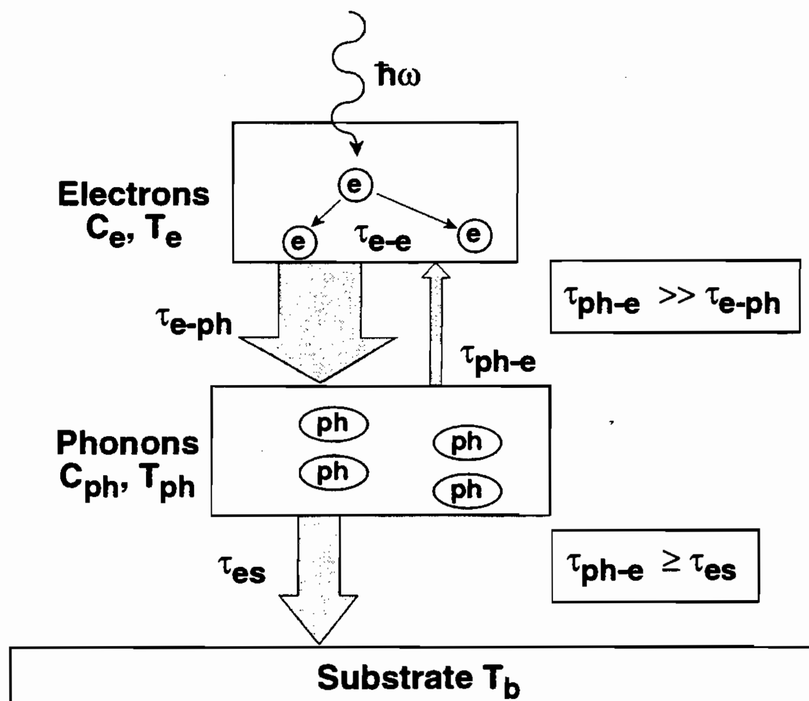

Fig. 4. Schematics of the energy flow diagram for the hot-electron effect.